Molecular Phylogenetics and Evolution 127 (2018) 723–731

Contents lists available at ScienceDirect

Molecular Phylogenetics and Evolution

journal homepage: www.elsevier.com/locate/ympev

# Prevalence of cryptic species in morphologically uniform taxa – Fast speciation and evolutionary radiation in Asian frogs

Zuyao Liu[a,b], Guoling Chen[a], Tianqi Zhu[c,d], Zhaochi Zeng[a], Zhitong Lyu[a], Jian Wang[a], Kevin Messenger[e], Anthony J. Greenberg[f], Zixiao Guo[b], Ziheng Yang[g], Suhua Shi[b,*], Yingyong Wang[a,*]

[a] The Museum of Biology, School of Life Sciences, Sun Yat-sen University, 510275 Guangzhou, China
[b] State Key Laboratory of Biocontrol and Guangdong Provincial Key Laboratory of Plant Resources, School of Life Sciences, Sun Yat-sen University, 510275 Guangzhou, Guangdong, China
[c] Institute of Applied Mathematics, Academy of Mathematics and Systems Science, Chinese Academy of Sciences, Beijing 100190, China
[d] Key Laboratory of Random Complex Structures and Data Science, Academy of Mathematics and Systems Science, Chinese Academy of Sciences, Beijing 100190, China
[e] Department of Zoology, Nanjing Forestry University, 210037 Jiangsu, China
[f] Bayesic Research, Ithaca, NY 14850 USA
[g] Department of Genetics, Evolution and Environment, University College London, London WC1E 6BT, UK

ARTICLE INFO

*Keywords:*
Cryptic species
Delimitation
Diversity
Megophrys
Phylogeography

ABSTRACT

Diversity and distributions of cryptic species have long been a vexing issue. Identification of species boundaries is made difficult by the lack of obvious morphological differences. Here, we investigate the cryptic diversity and evolutionary history of an underappreciated group of Asian frog species (*Megophrys*) to explore the pattern and dynamic of amphibian cryptic species. We sequenced four mitochondrial genes and five nuclear genes and delineated species using multiple approaches, combining DNA and mating-call data. A Bayesian species tree was generated to estimate divergence times and to reconstruct ancestral ranges. Macroevolutionary analyses and hybridization tests were conducted to explore the evolutionary dynamics of this cryptic group. Our phylogenies support the current subgenera. We revealed 43 cryptic species, 158% higher than previously thought. The species-delimitation results were further confirmed by mating-call data and morphological divergence. We found that these Asian frogs entered China from the Sunda Shelf 48 Mya, followed by an ancient radiation event during middle Miocene. We confirmed the efficiency of the multispecies coalescent model for delimitation of species with low morphological diversity. Species diversity of *Megophrys* is severely underappreciated, and species distributions have been misestimated as a result.

## 1. Introduction

Cryptic species are morphologically indistinguishable and mistakenly grouped as a single nominal species (Bickford et al., 2007). While they are hard to tell apart visually, these taxa diverge in their mating signals, interrupting gene flow. Acoustic and pheromones signals are typical in insects (Henry, 1994) and vertebrates, including bats (Jones and Barlow, 2004) and frogs (Narins, 1983). Additionally, species inhabiting extreme environments may be under selection for uniform morphology while maintaining ecological adaptations (Schönrogge et al., 2002). Since morphological characters are of no help in species delimitation in such taxa, molecular genetic data have been widely applied to discover cryptic species (Harrington and Near, 2011; Hedin, 2015; Satler et al., 2013). The multispecies coalescent model is the most popular among various approaches that leverage DNA sequence variation to diagnose species (Fujita et al., 2012). However, distinguishing between within-species population structure and among-species divergence remains a challenge (Sukumaran and Knowles, 2017). In addition, most studies delimit species only on the basis of molecular data. As speciation is a continuous process, it is hard to make a cut-off to identify the boundaries, especially when recent introgression is present (Wiens, 2007). Approaches that combine phenotypic and genotypic evaluations are thus potentially more fruitful than either method in isolation.

Here, we sought to explore the species boundaries and the dynamics of *Megophrys*. *Megophrys* species are widely distributed in the eastern and central Chinese mainland, throughout southeastern Asia, and extending to the islands of the Sunda Shelf and the Philippines (Fei et al.,

* Corresponding authors.
*E-mail addresses:* lssssh@mail.sysu.edu.cn (S. Shi), wangyy@mail.sysu.edu.cn (Y. Wang).

https://doi.org/10.1016/j.ympev.2018.06.020
Received 3 January 2018; Received in revised form 11 June 2018; Accepted 11 June 2018
Available online 18 June 2018
1055-7903/ 

2009; Li et al., 2014; Wang et al., 2014). Seven subgenera (Panophrys, Xenophrys, Ophyrophryne, Brachytarsophrys, Atympanophrys, Megophrys, and Pelobatrachus) are currently recognized as members of this genus, comprising approximately 70 species (Mahony et al., 2017; Orlov et al., 2015; Poyarkov Jr et al., 2017; Zhang et al., 2017). The taxonomic status of this group has been controversial due to a lack of molecular phylogenetic and comparative morphological studies (Delorme et al., 2006; Dubois and Ohler, 1998; Fei et al., 2009; Frost et al., 2006; Jiang et al., 2002; Khonsue and Thirakhupt, 2001; Li et al., 2011; Mahony et al., 2011; Ohler, 2003; Pyron and Wiens, 2011; Rao and Yang, 1997; Wang et al., 2012). Only two recent studies used comprehensive data to explore phylogenetic relationships within this group (Chen et al., 2017; Mahony et al., 2017).

Although horned frogs are reportedly widespread in southeastern China, many new species have been published in the past few years (Li et al., 2014; Poyarkov Jr et al., 2017; Wang et al., 2012; Wang et al., 2014; Zhao et al., 2014). Our long-term field investigations and recent publications suggest that the species diversity in this group is greatly underestimated. *Megophyrs* is not prone to dispersal and thrives only in specific habitats (Fei et al., 2009). Morphological similarity often hinders exact species recognition. This leads to misidentification of endemic species as geographic populations of a widely-distributed species, a problem only partially corrected in recent studies. Thus, the real distribution of these species remains to be determined, and it is reasonable to question the correctness of field records. To begin studying the evolutionary history and adaptation within the genus, it is necessary first to understand the phenotypic diversity and geographical distributions of *Megophrys* species.

In the present study, we delimit cryptic species using multiple approaches and confirm the results using morphological characters, revealing striking hidden diversity and distributional heterogeneity. Reconstruction of diversification history reveals an intriguing dispersal pattern of *Megophrys* and an ancient evolutionary radiation within the Panophrys group triggered by drastic climatic change and ancient hybridization. According to records and our results, *Megophrys* appears to be the most diverse amphibian group in China (Fei et al., 2009; Fei et al., 2010). Our results demonstrate the effectiveness of the multispecies coalescent model and emphasize the importance of sexual traits to confirm boundaries of cryptic species. Finally, we discuss the possibility of using cryptic groups such as Panophrys as new models to study patterns and dynamics of speciation and evolutionary radiation.

## 2. Material and methods

### 2.1. Sampling and PCR amplification

We sampled 293 individuals in total (Table S1 in Supplementary Material), including 243 from Panophrys, 23 from Xenophrys, 11 from Ophryophryne, six from Atympanophrys, and five from Brachytarsophrys. The extensive sampling of Panophrys was conducted to evaluate its evolutionary history. In addition, six individuals from *Leptolalax* were collected to use as an outgroup. All specimens were collected during field surveys from 2008 to 2016 (Fig. 1). Muscle tissues were collected in 95% ethanol for preservation. DNA was extracted from each muscle tissue sample using a standard extraction kit (Tiangen Biotech, Beijing, China). Four mitochondrial genes (16S, 12S, *CO1* and *CYTB*) and five nuclear genes (*CXCR-4*, *RAG-1*, *RAG-2*, *DISP-2* and *SALL-1*) were amplified in this study. Primers used in this study are listed in Supplementary Material, Table S2. PCR amplifications were performed in a 20 uL reaction volume with the following cycling conditions: an initial denaturing step at 95 °C for 4 min, 35 cycles of denaturation at 94 °C for 40 s, annealing at 45–53 °C for 40 s, extension at 72 °C for 1 min, and a final extension step of 72 °C for 10 min for mitochondrial genes. The *CXCR-4* gene was amplified using the protocol developed by Biju and Bossuyt, (2003). The other nuclear genes were amplified using a nested-PCR protocol (Shen et al., 2013). PCR products were purified using spin columns. The purified products were sequenced with both forward and reverse primers using the BigDye Terminator Cycle Sequencing Kit on an ABI Prism 3730 automated DNA analyzer according to the manufacturer's guidelines. All sequences were deposited in GenBank with accession numbers (Table S1 in Supplementary Material).

### 2.2. Phylogenetic analysis

Sequences were aligned in MEGA6 using the Clustal W algorithm with default parameters (Tamura et al., 2013). To compare our new sequences with ones downloaded from GenBank, we used seven genes


**Fig. 1. Sampling map**. Dots represent sampling localities. Numbers in dots correspond to locations listed in the Supplementary Material, Table S1.

(16S, 12S, *CXCR-4*, *RAG-1*, *RAG-2*, *DISP2* and *SALL-1*) to reconstruct the phylogenetic relationships among the anurans. Dataset containing eight genes (16S, 12S, *CO1*, *CYTB*, *RAG-1*, *RAG-2*, *DISP2* and *SALL-1*) was used to reconstruct the phylogenetic relationships among the *Megophrys*, and *CXCR-4* was excluded because of the missing information.

The anuran phylogeny was reconstructed with RaxML GUI 1.3 (Silvestro and Michalak, 2012) using the GTRGAMMA model with 1000 bootstrap replicates. *Megophrys* phylogenies were reconstructed using both a Maximum Likelihood (ML) and a Bayesian inference (BI) method to infer the phylogenies. We concatenated the four mitochondrial fragments and treated them as a single locus. The four nuclear fragments were divided into 12 partitions according to codon type. Following a previous study (Pyron and Wiens, 2011), *L. laui*, *L. liui*, and *L. alpinus* were used as outgroups. Best nucleotide substitution models are listed in Supplementary Material, Table S3. The ML bootstrap consensus tree was inferred from 1000 replicates using RaxML GUI 1.3 (Silvestro and Michalak, 2012). BI phylogenetic trees were constructed using MrBayes 3.2.4 (Ronquist et al., 2012). With a sampling frequency of 1000, the number of samples was 5 million generations for mitochondrial and 10 million generations for nuclear genes. The first 25% of samples was discarded as burn-in. We ensured convergence by conducting two replicate analyses and requiring that the potential scale reduction factor (PSRF) value be less than 0.01 and the effective sample size (ESS) value larger than 200 (calculated using Tracer v1.4).

### 2.3. Estimation of species diversity

We used three approaches (ABGD, GMYC and bPTP) to delimit species boundaries and BPP to validate the delineation. First, we calculated pairwise genetic distance using the K80 model (Kimura, 1980) in MEGA6. The genetic distance matrix was used as input to the Automatic Barcode Gap Discovery web server (ABGD) (http://wwwabi.snv.jussieu.fr/public/abgd/) (Puillandre et al., 2012). Second, we used a Bayesian implementation of the Poisson Tree Processes model (bPTP) (Zhang et al., 2013) on the web server (http://species.h-its.org/ptp/). The bPTP model is a tree-based method distinguishing populations and species under a coalescent model. The branch lengths represent mutations, used for simulating coalescence and speciation events. Third, mitochondrial genes were used to reconstruct an ultra-metric tree with BEAST v 2.4.4 (Bouckaert et al., 2014). Once that was accomplished, the General Mixed Yule-Coalescent (GMYC) approach (Pons et al., 2006) was used to delimit species utilizing the 'splits' R package (Ezard et al., 2009). The GMYC model is another tree-based method using a coalescent model. It delimits species boundaries by optimizing the set of nodes defining transitions between interspecific and intraspecific processes.

To validate the species delineations, we used BPP (analysis A10) (Rannala and Yang, 2013; Yang, 2015; Yang and Rannala, 2010). We separated the species tree into five sub-trees according to the major clades (Fig. 3) to reduce computation time. Each analysis was run twice to check for convergence. The number of samples was 150,000 with sampling frequency 10; the first 50,000 samples were discarded as burn-in.

### 2.4. Mating calls and morphological analyses

We analyzed mating calls and morphological characters for each species. Mating calls were recorded under natural conditions using the Sony PCM-D100 Linear PCM Recorder. Subsequent analyses were conducted in Raven Pro 1.5 (Program, 2014). Sound files were digitized and visualized as spectrograms for analysis. We recorded 29 calls and exported the spectrograms. In addition, seven measurements were extracted for comparison. Each measurement included 10 syllables and intervals. Mean values and standard deviations were calculated for comparison. Morphological characters including seven measurements were used to distinguish species. External measurements included snout-vent length (SVL), tibial length (TIB), tubercle on upper eyelids, vomerine teeth, notched tongue, lateral fringes on toes, and webbed toes.

### 2.5. Species tree and divergence-time estimation

We estimated the age of the Megophryidae root using MCMCTree, combining fossils and geographical events to calibrate the tree (Yang, 2007). We used the same fossil combination as Mahony et al. (2017) (Table S4 in Supplementary Material). Because only one fossil was available for each calibrated node, it was used as a soft minimum bound. The soft maximum bounds were set at the estimated 95% credible intervals (CI) from previous studies (San Mauro et al., 2005; Roelants et al., 2007; Kurabayashi et al., 2011; Pyron, 2014; Mahony et al., 2017). If both a fossil record and geographical event were available, we used the information to set soft minimum and maximum bounds. If a fossil date fell within a geological time period, we used the fossil age as the soft minimum bound and the beginning of the geological event as the soft maximum bound. Otherwise, we set both bounds at the geological event boundaries. We assumed the HKY + G model of nucleotide substitution and the independent model to relax the clock. The substitution rate ($\mu$) and the rate-drift parameter ($\sigma^2$) were assigned gamma priors, $\mu \sim G(1, 10)$ with mean $0.1 * 10^{-8}$ substitutions per site per year and $\sigma^2 \sim G(1, 3)$ with mean 1/3. The priors and the calibrations match those of Mahony et al. (2017). The burn-in was 50,000 generations. We sampled the MCMC chains every 10 steps for a total of 20,000 samples. The analysis was conducted twice to ensure MCMC chain convergence. To test if the priors were influencing our conclusions, we also conducted the analyses using more diffuse priors, with $\mu \sim G(0.1, 1)$ and $\sigma^2 \sim G(0.1, 0.3)$.

Having dated the root, we estimated divergence times and the species tree in *BEAST (Bouckaert et al., 2014). We used data from four mitochondrial and four nuclear genes. We arranged the dataset into 13 partitions: one mitochondrial and 12 nuclear. The uncorrelated log-normal model was used to relax the clock. The root age of the family Megophryidae estimated from MCMCTree was used as the root age prior. We ran five independent analyses and sampled 2 billion iterations in each with sample frequency of 20,000 steps. Convergence was diagnosed using Tracer v1.4.

### 2.6. Ancestral area reconstruction

We used two models, Dispersal-Extinction-Cladogenesis (DEC) and Bayes-DEC (S-DEC) in RASP 3.2 (Yu et al., 2015) to perform ancestral area reconstruction. Areas were divided into four parts on the basis of topography: (A) the third step of Chinese topography, the region stretching from the Xuefeng and Wu mountains to the East and South coasts (average elevation of 500 m); (B) northern regions of Myanmar, Vietnam, Laos, and Thailand, as well as the second step of Chinese topography (eastern Qinghai-Tibetan plateau to Xuefeng and Wu mountains; average elevation of 1500 m); (C) northern Cambodia, central and southern Vietnam, and Laos; (D) Nepal, Indian Himalayas, Bhutan, eastern Bangladesh, and western Myanmar. The geographic design was based on the topography of east Asia. Areas A, B and C were separated by lines of mountains, and area D was separated from the other by the Qinghai-Tibetan plateau. Species distributions were inferred from the combination of our field surveys and the literature (Frost, 2016). Only reliable records were taken into consideration. If the species occurred on the boundaries of adjacent regions, we assigned the species to both regions. The species tree estimated using *BEAST was treated as input in both analyses. Since we lacked Xenophrys and Ophryophryne samples from Southeast Asia, we constrained the ancestral range of these two groups (species) according to the results of a previous large-scale analysis (Mahony et al., 2017).

### 2.7. Diversification and speciation

To explore the accumulation of lineages, we drew a Lineage-Through-Time (LTT) plot in Tracer v1.4. We also used BAMM (Bayesian Analysis of Macroevolution Mixtures) version 2.5 (Rabosky et al., 2013) and BAMMtools 2.5 (Rabosky et al., 2014b), which can explicitly model variation of diversification rates along the tree, to explore speciation rates on the phylogeny. BAMM uses a reversible jump Markov Chain Monte Carlo method to explore the universe of models that differ in the number of distinct evolutionary regimes (Rabosky et al., 2014a). Taking the factor of incomplete and non-random sampling into consideration, we allowed individual clades to have different sampling probabilities. We set the probability to 1.0 for Panophrys. We removed the Panophrys species and re-calculated the probability for Xenophrys. Probabilities for other groups were calculated based on records from the literature. Because of the small number of tips in the species tree, we assigned the prior on the expected number of shifts to 1.0. BAMM was run for 10 million iterations, and samples were recorded every 1000 steps. In addition to plotting the speciation rate across the whole species tree, we isolated the Panophrys clade for a separate calculation. We also removed this set of taxa from the data set and re-ran the analyses without it. We further performed a macro-evolutionary cohort analysis using BAMMtools, providing a summary of the extent to which species share a common macro-evolutionary rate dynamic (Rabosky et al., 2014a).

### 2.8. Distinguishing hybridization and incomplete lineage sorting

Cyto-nuclear discordance can be caused by incomplete lineage sorting (retention of ancestral polymorphism) or by hybridization (Renoult et al., 2009). If hybridization occurs, parental nuclear genes can undergo recombination and create intermediate haplotypes. To distinguish hybridization from incomplete lineage sorting, we applied an approach developed by Joly (2012). If the discordance between the gene and species trees is due to incomplete lineage sorting, coalescence time of DNA sequences should be earlier than species divergence time (looking forward in time). If this pattern can be rejected, we can infer the existence of historical hybridization (Joly et al., 2009). We therefore tested the discordance between mitochondrial and nuclear DNA in the Panophrys group assuming no hybridization. 50 sequences were randomly picked from the whole dataset and at least one sequence per species was included. We grouped our 50 mitochondrial sequences into five categories (I-V) using the nuclear DNA-based phylogeny (Fig. S2 in Supplementary Material). Group I includes 14 sequences, group II 13, group III nine, group IV eight, and group V six. We then used the JML program to test for hybridization (Joly, 2012). JML combines code for gene-tree simulation from MCMCcoal (Rannala and Yang, 2003) and sequence simulation from Seq-gen 1.3.2 (Rambaut and Grass, 1997). We simulated 3600 gene trees from the species tree under the assumption of no hybridization, and then used the gene trees to simulate alignments. By comparing the minimum uncorrelated pairwise distances between the simulated and observed data, we can assess evidence for past hybridization.

## 3. Results

### 3.1. The Megophrys phylogeny

The mitochondrial trees produced by the two methods are approximately congruent in topology (Fig. S1 in Supplementary Material). Samples from Brachytarsophrys (Bootstrap value = 100 BV hereafter, Posterior probability = 1.00 PP hereafter), Atympanophrys (BV = 95, PP = 1.00), Ophyrophryne (BV = 100, PP = 1.00), Xenophrys (BV = 98, PP = 1.00), and Panophrys (BV = 95, PP = 1.00) are monophyletic, consistent with previous results (Chen et al., 2017). Using nuclear gene data, we obtained a generally similar phylogeny, irrespective of the inference method used (Fig. S2 in Supplementary Material). While some node support values are not high, the consistency between the datasets enhances our confidence that the estimated phylogenies generally correctly reflect evolutionary relationships. The position of Ophryophryne in our tree is consistent with Mahony et al. (2017), and different from Chen et al. (2017), where it forms a clade with Xenophrys.

**Table 1**
JML analysis of the mitochondrial dataset consisting of 50 sequences representing clade I to V. For each sequence pair the method calculates the observed nucleotide distance and the probability of observing this distance if no hybridization took place.

| Comparison | minimum observed distance | Probability |
|---|---|---|
| I vs II | 0.072 | < 0.001 |
| I vs III | 0.081 | < 0.001 |
| I vs IV | 0.068 | < 0.001 |
| I vs V | 0.065 | < 0.001 |
| II vs III | 0.064 | < 0.001 |
| II vs IV | 0.056 | < 0.001 |
| II vs V | 0.078 | < 0.001 |
| III vs IV | 0.069 | < 0.001 |
| III vs V | 0.087 | < 0.001 |
| IV vs V | 0.071 | < 0.001 |

While the nuclear and mitochondrial trees largely agree, we do find some conflicts, particularly at the tips of the dendrogram. Such patterns can arise either due to incomplete lineage sorting or hybridization upon secondary contact among newly-formed species. Using incomplete lineage sorting as a null hypothesis, we conducted an analysis using JML. Our results (Table 1) reject the null hypothesis with high confidence in each Panophrys clade, suggesting potential past hybridization among species of this group.

### 3.2. Species delimitation

We used three methods (ABGD, GMYC and bPTP) to estimate the number of species in our sample and to assign individuals to species (Fig. 2a). Setting the barcoding gap at 2.1%, the ABGD method identified 70 species. The GMYC approach, used with a single threshold, allows for a likelihood ratio test against a null model where all samples belong to a single species. The likelihood value is 513.73 ($p < 0.01$), strongly rejecting the null model (null likelihood value = 490.00). The model estimates that there are 82 species in our data set. Finally, the bPTP analysis estimates the number of species at 85, with support values ranging from 0.70 to 1.00.

Treating the known species as independent taxonomic units and taking a consensus of the three delineation methods, we estimate the total number of species at 78 (including outgroup species). This gives us 43 new species. We used the BP&P program to test our results. All but two taxa are validated with posterior probabilities larger than 0.95. The exceptions are *M.* sp39 and *M.* sp40, whose posterior probability is 0.85. Among the new cryptic species, only two belong to clades B or C. All others are in clade A, mostly found in southern and eastern China (Fig. 3).

Our morphological analyses suggest a barrier to gene flow among the newly-identified cryptic species (Tables S5 and S6 in Supplementary Material). The results show extensive differences and support our DNA phylogeny-based species delimitation. In addition, sympatric species appear to exhibit particularly striking mating-call divergence and morphological differences (Fig. 2b and Table 2).

### 3.3. Divergence time and species-tree estimation

With new species assignments in hand, we proceeded to estimate divergence times on the species phylogeny. Using a diverse sample of anuran and outgroup species, we ran MCMCTree and found that the divergence time between Anura and Caudata is about 273 million years

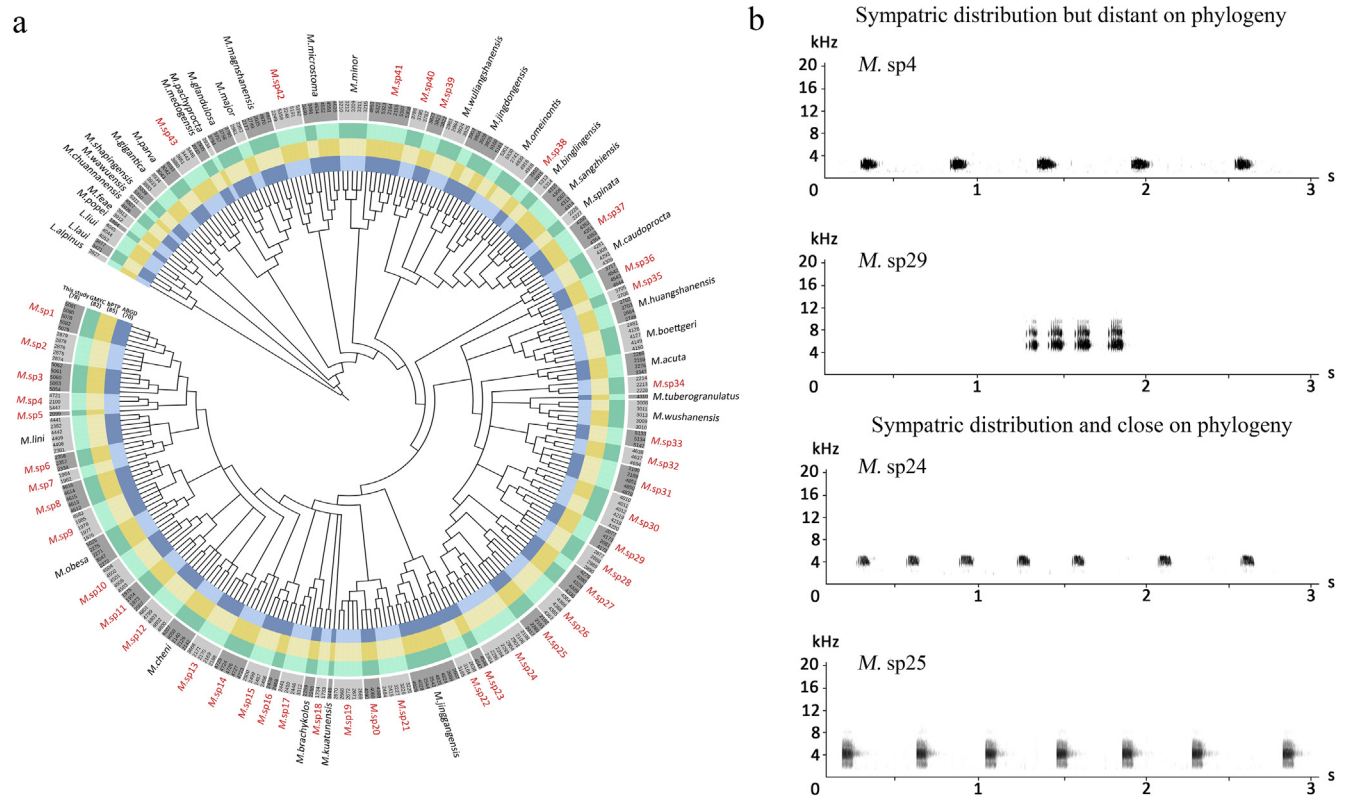


**Fig. 2. Species delimitation and acoustic comparison of *Megophrys*.** (a) *Megophrys* species delimitation. The ultrametric tree is reconstructed using Bayesian inference. Circles from inside to outside represent the results form ABGD, bPTP, and GMYC methods. Samples belonging to the same species are shaded in an alternating pattern. The grey outermost circle indicates the consensus of three approaches. Each lineage number corresponds to the specimen voucher. Cryptic species are marked in red. (b) Mating call spectra of sympatric species. (For interpretation of the references to color in this figure legend, the reader is referred to the web version of this article.)

ago (Mya), with the 95% credible interval (CI) (243.18, 329.54) (Fig. S4 in Supplementary Material). The time to the most recent common ancestor (TMRCA) of the *Megophrys* genus is 93 Mya (74, 115).

Moving inside the *Megophrys* clade, we used *BEAST to estimate among-species relationships and divergence times. We recover the previously-identified five groups (Panophrys, Ophyrophryne, Xenophrys, Brachytarsophrys, and Atympanophrys), consistent with individual DNA sample trees (Fig. 3). The TMRCA of Panophrys, the clade that includes most cryptic species, is 27 (19, 39) Mya (clade B in Fig. 3). Among the subclades within Panophrys, a major diversification event occurred 19 (17, 24) Mya (clade AB in Fig. 3). The TMRCA of Panophrys and Ophryophryne (clade BC) is 37.5 (22, 53) Mya, and the TMRCA of Panophrys, Ophryophryne and Xenophrys (clade BCD) is 40 (24, 57) Mya. The most closely related species (*M. sp15* and *M. sp16*) split 0.22 Mya, and the second closest (*M. medogensis* and *M. pachyproctus*) separated 1.38 Mya. Divergence times of other species exceed 2 Mya.

### 3.4. Ancestral-area reconstruction

Starting with the species phylogeny, we attempted to reconstruct ancestral ranges of clades using RASP v3.2 software. We estimate that dispersal events and vicariance events are necessary to explain the current species distribution (Fig. 3). The MRCA of Atympanophrys and Brachytarsophrys was present in a region encompassing northern Myanmar, northern Vietnam and Laos, and the second step of Chinese topography. Only *M. popei* dispersed to the third step of Chinese topography. A previous study (Mahony et al., 2017) suggested that Xenophrys originated in the region that includes Nepalese and Indian Himalayas, Bhutan, eastern Bangladesh, and western Myanmar (we call this “region D” in Fig. 3), and later dispersed to region B. The split between Panophrys and Ophryophryne was clearly due to a vicariance event, probably the orogenic movement of the Truong Son Mountains. This mountain range forms a barrier between the dry highlands of the central Indochina peninsula and wet lowlands of Vietnam to the south (Che et al., 2010). Our results reveal that the MRCA of Panophrys lived in region B and dispersed to region A, suggesting that a vicariance event dividing region A and B occurred 20 Mya. Taking our species delimitation results into consideration, most speciation events occurred after the A-B vicariance, indicating that an ancient radiation event happened in east and south China. Our analyses are not sufficient to resolve the complex history of clades belonging to the Panophrys group. The weak support for phylogenetic relationships among lineages within this clade makes ancestral-range analyses unreliable.

### 3.5. Historical diversification

Bayesian Analysis of Macroevolution Mixtures (BAMM) can estimate evolutionary rate variation through time and among lineages. We employed this method to study our data set and found a major increase in speciation rate at the base of the clade that includes most southern and eastern species of Panophrys. We estimate that the rate increase happened about 20 Mya, and corresponds to the very short branches on the phylogeny (colored red in Fig. 4a, upper panel). Looking at the speciation rate using a Lineage-Through-Time (LTT) plot (Fig. 4a, lower panel), we observe an inflection point between about 20 and 15 Mya, suggesting a past radiation event.

To examine the contribution of the Panophrys clade to the potential radiation event, we analyzed this group of taxa and species belonging to all other branches separately. Speciation-rate estimates for the whole data set show an increase between 20 and 10 Mya, as discussed above (Fig. 4b, top panel). This increase completely disappears if we exclude

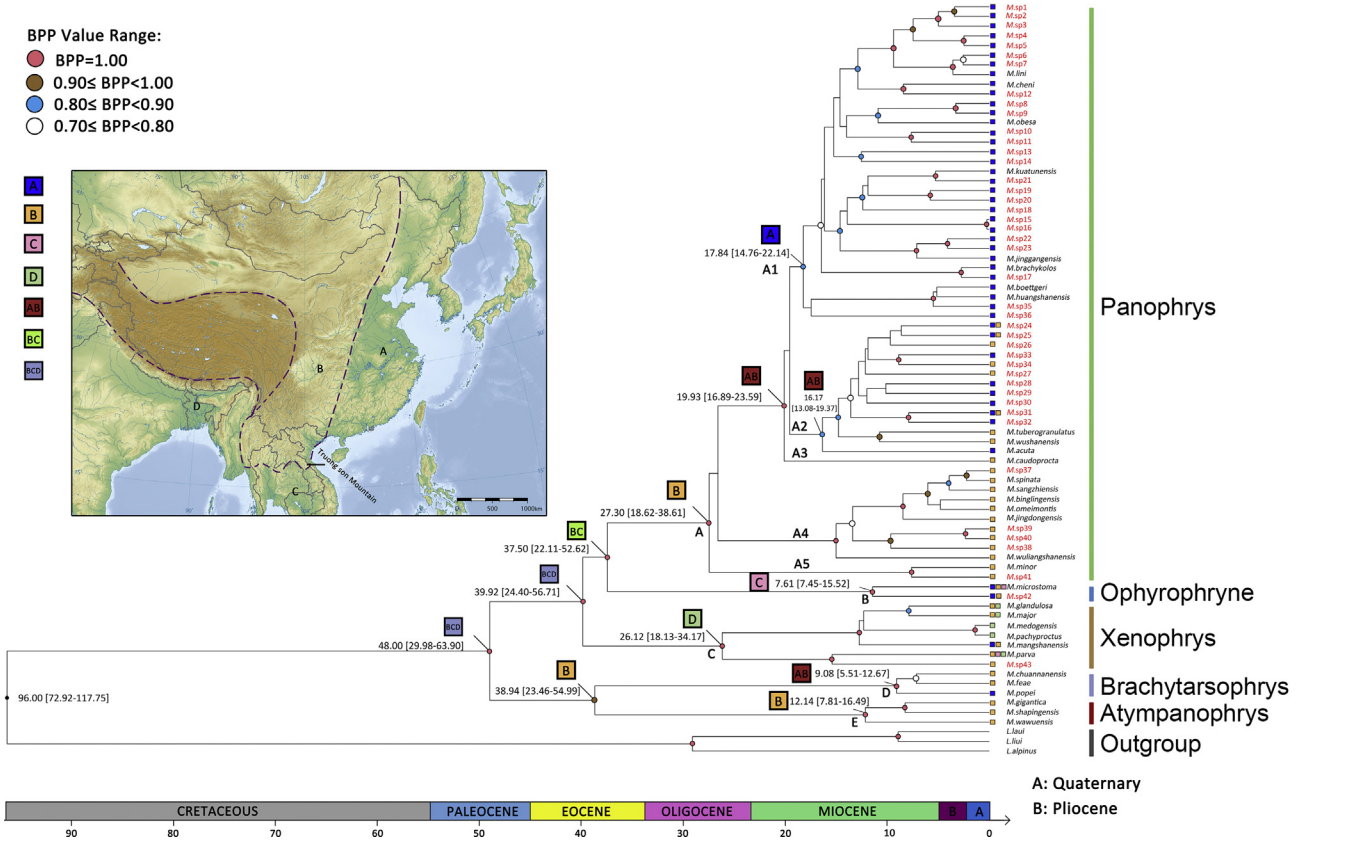


**Fig. 3. Chronogram and the *Megophyrs* species tree.** Time units are in millions of years. Dots on each node reflect BPP values. Colored squares after lineages represent species distributions. Five major clades are labeled with letters (A–E). Divergence times of major lineages are marked with 95% CI in brackets. Map (top left) shows the four regions: (A) the third step of Chinese topography, the region stretching from the Xuefeng and Wu Mountains to the east and south coasts (average elevation 500 m); (B) northern Myanmar, Vietnam, Laos and Thailand, and the second step of Chinese topography (average elevation of 1500 m); (C) northern Cambodia, central and southern Vietnam, and Laos; (D) Nepal-Indian Himalayas, Bhutan, eastern Bangladesh, and western Myanmar. (For interpretation of the references to color in this figure legend, the reader is referred to the web version of this article.)

Panophrys (Fig. 4b, bottom panel). However, it grows in prominence when that clade is analyzed by itself (Fig. 4b, middle panel). This divergence of speciation-rate dynamics between Panophrys and the other *Megophrys* species can also be visualized using a macro-evolutionary cohort display (Fig. S5 in Supplementary Material), a plot that groups species by historical evolutionary rate similarity. Taken together with the striking mating-call divergence, our results strongly suggest that the ancient speciation events can be regarded as a radiation.

## 4. Discussion

### 4.1. Phylogeny and cryptic diversity of Megophrys

We undertook a comprehensive evaluation of the *Megophrys* phylogeny. Only recently (Chen et al., 2017; Mahony et al., 2017) have any attempts to tease apart the complex relationships in this clade been published, and the conclusions so far are contradictory in key respects. The focus of controversy is the validity of genus-level rank of seven groups: Panophrys, Xenophrys, Ophryophryne, Brachytarsophrys, Atympanophrys, Megophrys, and Pelobatrachus. Our molecular phylogeny agrees with that of Mahony et al. (2017). In addition to a molecular phylogeny, morphological differentiation is considered necessary to assign genus-level status to taxa. Given that only Atmpanophrys, Brachytarsophrys, and Ophryophryne have unique characters, we tentatively apply the taxonomy proposed by Mahony et al. (2017) that recognizes all the Asian horned frogs as a single genus with seven subgenera. Further study on morphological characters is needed to corroborate these conclusions.

The consensus of different methods suggests that there are ~78 species in our sample, including outgroups. We found 43 cryptic taxa,

**Table 2**
Morphological comparison of sympatric species.

| Species | SVL (mm) | TIB: SVL | Horn-like tubercle at edge of upper eyelid: long point (++), slightly large (+), absent or indistinct (−) | Vomerine teeth: present (+) or absent (−) | Tongue: notched (++), feebly nothced (+) or not notched (−) | Lateral fringes on toes: wide (++), narrow (+), lacking (−) | Toes: at least one-fourth webbed (+++), one-fourth webbed (++), with rudiment of web (+), or without web (−) |
|---|---|---|---|---|---|---|---|
| *Sympatric distribution but distant on phylogeny* | | | | | | | |
| *M.* sp4 | 35.1–37.3 | 0.46–0.47 | − | + | − | − | + |
| *M.*sp29 | 25.5–31.0 | 0.46–0.54 | + | + | − | + | + |
| *Sympatric distribution and close on phylogeny* | | | | | | | |
| *M.*sp24 | 28.9–33.2 | 0.46–0.52 | + | − | − | − | + |
| *M.*sp25 | 55.8–61.8 | 0.45–0.47 | ++ | − | − | + | ++ |

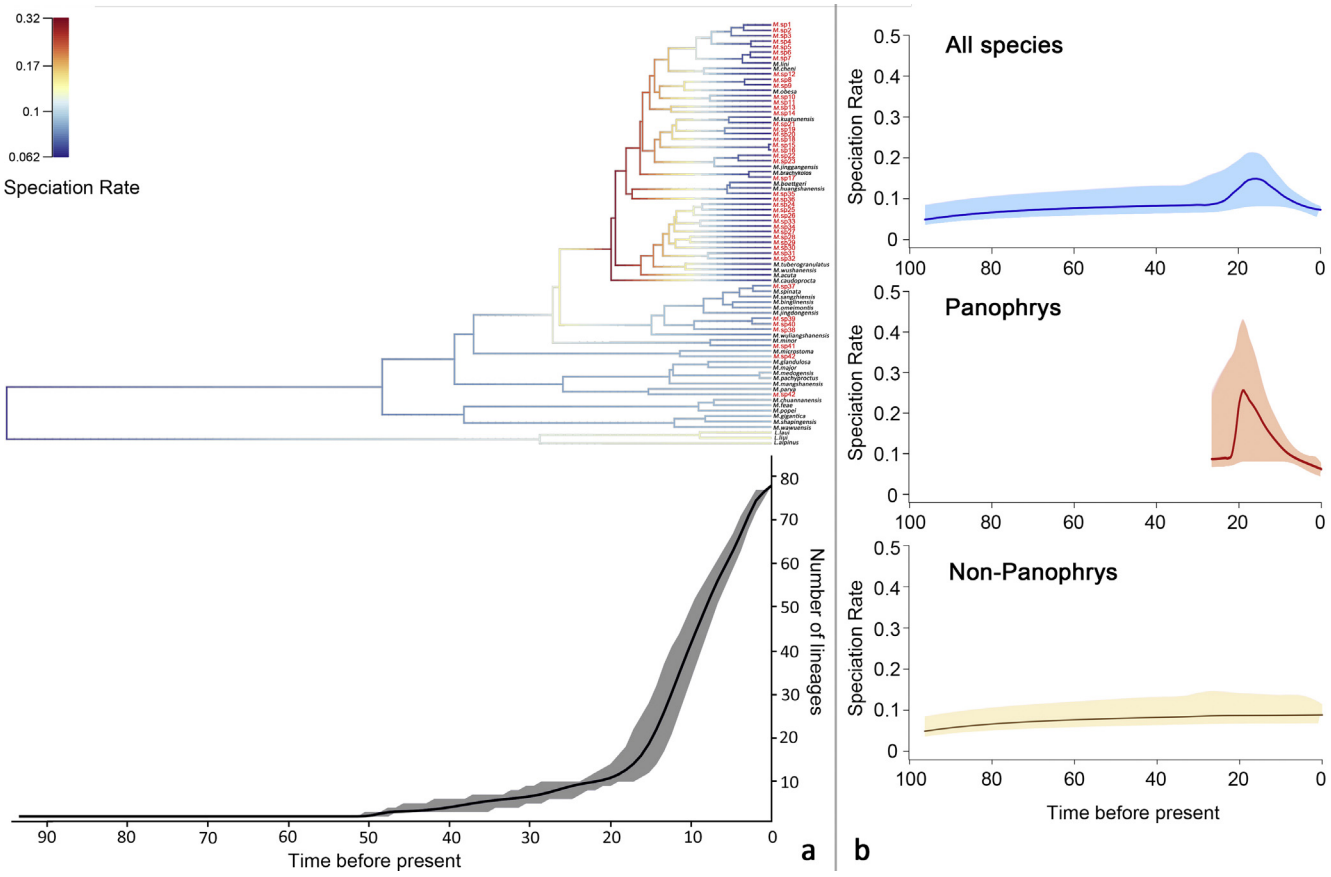


**Fig. 4. *Megophrys* diversification and speciation rates.** (a) speciation rate (speciation events per lineage per million years) along the phylogeny (rates reflected in branch colors as indicated, upper panel). Mean number of lineages as a function of time (lower panel). Gray region reflects the 95% CI. (b) Speciation rates through time, analyzed from three data sets. Lines represent means and lighter shadows delimit 95% CI. (For interpretation of the references to color in this figure legend, the reader is referred to the web version of this article.)

41 of which belong to the Panophrys subgenus. We confirmed these phylogenetic estimates with a study of mating-call and morphological character divergence. Our results indicate that sequence divergence was accompanied by pre-mating reproductive isolation.

China is the largest and most geographically diverse country in Asia. As such, it is rich in species diversity with high levels of endemism (Caldecott et al., 1996). Particularly, it is estimated that China is fifth in the world when it comes to amphibian diversity (Xie et al., 2007). However, our results suggest that this diversity is still understudied and potentially severely underestimated. In the Panophrys subgenus alone, we found 158% more species than the 26 previously recognized. It should be noted that our results might underestimate the real species diversity of Panophrys because we were unable to collect samples in some parts of southeastern China.

The correspondence of new cryptic species with geographical locations leads us to re-evaluate previously-accepted distributions. For example, *M. brachykolos* was considered to be wide-spread, with the northernmost record in south Hubei and the westernmost record in east Guangxi (Fei et al., 2010; Frost, 2016). However, once we take into account the newly-identified taxa, only the populations in Hong Kong (the type locality) appear to be the real *M. brachykolos*. Another convincing example is *M. kuatunensis*, whose southernmost record was thought to lie on the south coast of west Guangdong and the northernmost record on the east coast of Zhejiang (Fei et al., 2010; Frost, 2016). However, the actual distribution of this species, according to our results, is limited to the Guadun county in Fujian.

Sympatric distribution is very common in the Panophrys subgenus. For instance, *M. acuta* and *M. obesa* both inhabit the Heishiding Nature Resever, *M. boettgeri* and *M. kuatunensis* are both found in Guadun county, and *M. jinggangensis*, *M. lini*, and *M. cheni* all inhabit the Jinggangshan Nature Reserve (Table S1 in Supplementary Material). Although similar in appearance (but not mating calls), these sympatric species are usually far from each other on the phylogenetic tree, suggesting multiple colonization events and secondary contact.

### 4.2. Cryptic species delineation

Identifying species boundaries has been a challenge (Balakrishnan, 2005). Traditional approaches based on morphological characters often fail at species delimitation, especially for cryptic species. Various approaches have been developed and discordance across results is often reported from these methods (Carstens et al., 2013). Therefore, it is advisable to integrate multiple data sources when diagnosing species. Weak mobility and high specificity to particular environments produced high levels of allopatry among populations of *Megophrys*. Thus, recent gene flow, one of the main causes of species delineation failure, is unlikely. Adding mating-call measurements to DNA sequence data, we demonstrate that the species (particularly sympatric ones) identified in this study evolved reproductive isolation. Some morphological characters also diverge between our putative species, further supporting our proposed species boundaries. In the absence of obvious morphological divergence, differences in life history, distribution, environmental conditions and mating signals are particularly pivotal for inference.

Our results suggest that the multispecies coalescent model is effective for species delineation in the absence of recent migration. Excluding the influence of recent gene flow, the multispecies coalescent model outperforms distance-based approaches. In general, this model is

suitable for at least a tentative identification of cryptic groups with no recent gene flow when no ecological or morphological data are accessible. However, caution is warranted and independent lines of evidence should be used, if possible, to corroborate inferences from the multi-species coalescent.

### 4.3. Interacting processes stimulate evolutionary radiations

Five distinct *Megophrys* subgenera follow an intriguing geographical distribution pattern. Our analyses indicate that all extant Panophrys, Xenophrys, Ophrophryne, Brachytarsophrys, and Atympanophrys in China originated from Southeast Asia. The forces of dispersal and vicariance have shaped the modern distribution and diversity of these genera. The *Megophrys* TMRCA is about 48 Mya, coinciding with the India-Asia collision that caused the still rising Qinghai-Tibetan plateau (Zhu et al., 2005). This geological event shaped the present varied topography of China, with high mountains, valleys, and plateaus. Dispersal played an important role in the evolutionary history of Atympanophrys and Brachytarsophrys. Our results reveal that the ancestral populations of Atympanophrys lived in southwest China and later dispersed to the edge of the Sichuan Basin. Some ancestral populations of Brachytarsophrys dispersed along the south edge of the Sichuan Basin, while others emigrated to the Qinghai-Tibetan plateau (the highest ground in the area with average elevation of 4000 m) along the Hengduan mountains. Geographical dispersal patterns of the Panophrys subgenus are intriguing if we consider the likely radiation event that occurred in this clade. Our results indicate that Panophrys originated in the region east of the Qinghai-Tibetan plateau and dispersed to Xuefeng mountains and southeast China. Interestingly, although the elevation of the Qinghai-Tibetan plateau is a constant process, there have been six accelerations since Miocene, and one of them occurred between 25 and 20 Mya (An et al., 2006). The resulting orogenesis created geographical barriers for these species. In addition, the rise of the Qinghai-Tibetan plateau caused a violent and rapid shift in climate to a monsoon-dominated pattern (Guo et al., 2002). This may have given an additional impetus to rapid speciation within Panophrys. This appears to coincide with the evolutionary radiation event that we estimated from DNA data, suggesting the possibility of the acceleration of speciation. Our cohort analysis further confirms this scenario by identifying a distinct speciation-rate regime for this group of lineages.

## 5. Data accessibility

Sequences are deposited on GenBank (Table S1 in Supplementary Materials).

## Acknowledgements

We thank Jian Zhao, Yulong Li, Hailong He, and Runlin Li from the Museum of Biology, Sun Yat-sen University, and Jianhuan Yang from the Kadoorie Farm and Botanic Garden for their help with fieldwork.

## Funding

This work was supported by the Comprehensive Scientific Survey of the Luoxiao Range Region in China (2013FY111500); the National Natural Science Foundation of China (grant numbers 11201224, 11301294, 31301093, 31600182, 31671370, 41130208, 91331202 and 91731301); the 985 Project (grant 33000-31131105); National Key Research and Development Plan (2017FY100705) and a grant from the Youth Innovation Promotion Association of the Chinese Academy of Sciences (2015080).

## Author contribution

Y.Y. W and S.H.S conceived and designed the experiments; Z.Y.L, G.L.C, Z.C.Z, Z.T.L, J.W, K.M, and Y.Y.W collected materials; Z.Y.L and G.L.C performed experiments; Z.Y.L and T.Q.Z analyzed the data; Z.Y.L wrote the manuscript; S.H.S, T.Q.Z, Y.Y.W, Z.X.G, A.J.G and Z.H.Y revised the manuscript.

## References

An, Z.-S., Zhang, P.-Z., Wang, E.-Q., Wang, S.-M., Qiang, X.-K., Li, L., Song, Y.-G., Chang, H., Liu, X.-D., Zhou, W.-J., 2006. Changes of the monsoon-arid environment in China and growth of the Tibetan Plateau since the Miocene. Quat. Sci. 26, 678–693.
Balakrishnan, R., 2005. Species concepts, species boundaries and species identification: a view from the tropics. System. Biol. 54, 689–693.
Bickford, D., Lohman, D.J., Sodhi, N.S., Ng, P.K., Meier, R., Winker, K., Ingram, K.K., Das, I., 2007. Cryptic species as a window on diversity and conservation. Trends Ecol. Evol. 22, 148–155.
Biju, S., Bossuyt, F., 2003. New frog family from India reveals an ancient biogeographical link with the Seychelles. Nature 425, 711–714.
Bouckaert, R., Heled, J., Kühnert, D., Vaughan, T., Wu, C.-H., Xie, D., Suchard, M.A., Rambaut, A., Drummond, A.J., 2014. BEAST 2: a software platform for Bayesian evolutionary analysis. PLoS Comput. Biol. 10, e1003537.
Caldecott, J., Jenkins, M., Johnson, T., Groombridge, B., 1996. Priorities for conserving global species richness and endemism. Biodivers. Conserv. 5, 699–727.
Carstens, B.C., Pelletier, T.A., Reid, N.M., Satler, J.D., 2013. How to fail at species delimitation. Mol. Ecol. 22, 4369–4383.
Che, J., Zhou, W.-W., Hu, J.-S., Yan, F., Papenfuss, T.J., Wake, D.B., Zhang, Y.-P., 2010. Spiny frogs (Paini) illuminate the history of the Himalayan region and Southeast Asia. Proc. Natl. Acad. Sci. 107, 13765–13770.
Chen, J.-M., Zhou, W.-W., Poyarkov, N.A., Stuart, B.L., Brown, R.M., Lathrop, A., Wang, Y.-Y., Yuan, Z.-Y., Jiang, K., Hou, M., 2017. A novel multilocus phylogenetic estimation reveals unrecognized diversity in Asian horned toads, genus *Megophrys* sensu lato (Anura: Megophryidae). Mol. Phylogenet. Evol. 106, 28–43.
Delorme, M., Dubois, A., Grosjean, S., Ohler, A., 2006. Une nouvelle ergotaxinomie des Megophryidae (Amphibia, Anura). Alytes 24, 6–21.
Dubois, A., Ohler, A., 1998. A new species of *Leptobrachium* (Vibrissaphora) from northern Vietnam, with a review of the taxonomy of the genus *Leptobrachium* (Pelobatidae, Megophryinae). Dumerilia 4, 1–32.
Ezard, T., Fujisawa, T., Barraclough, T., 2009. Splits: species' limits by threshold statistics. R package version 1.
Fei, L., Hu, S., Ye, C., Huang, Y., 2009. Fauna Sinica. Amphibia vol. 2 Anura. Science Press, Beijing.
Fei, L., Ye, C., Jiang, J., 2010. Colored Atlas of Chinese Amphibians. Sichuan Publishing House of Science and Technology, Chengdu, pp. 1–519.
Frost, D., 2016. Amphibian Species of the World: an Online Reference. Version 6.0. American Museum of Natural History, New York.
Frost, D.R., Grant, T., Faivovich, J., Bain, R.H., Haas, A., Haddad, C.F., De Sa, R.O., Channing, A., Wilkinson, M., Donnellan, S.C., 2006. The amphibian tree of life. Bull. Am. Museum Nat. History 1–291.
Fujita, M.K., Leaché, A.D., Burbrink, F.T., McGuire, J.A., Moritz, C., 2012. Coalescent-based species delimitation in an integrative taxonomy. Trends Ecol. Evol. 27, 480–488.
Guo, Z., Ruddiman, W.F., Hao, Q., Wu, H., Qiao, Y., Zhu, R.X., Peng, S., Wei, J., Yuan, B., Liu, T., 2002. Onset of Asian desertification by 22 Myr ago inferred from loess deposits in China. Nature 416, 159–163.
Harrington, R.C., Near, T.J., 2011. Phylogenetic and coalescent strategies of species delimitation in snubnose darters (Percidae: Etheostoma). Systemat. Biol. 61, 63–79.
Hedin, M., 2015. High-stakes species delimitation in eyeless cave spiders (*Cicurina*, Dictynidae, Araneae) from central Texas. Mol. Ecol. 24, 346–361.
Henry, C.S., 1994. Singing and cryptic speciation insects. Trends Ecol. Evol. 9, 388–392.
Jiang, J., Fei, L., Zheng, M., Ye, C., Xie, F., Chen, Y., 2002. Description of *Megophrys wawuensis* (Anura, Pelobatidae) from Sichuan, China, with discussion on the relationships of its related species. Cultum Herpetol. Sin. 9, 80–87.
Joly, S., 2012. JML: testing hybridization from species trees. Mol. Ecol. Resour. 12, 179–184.
Joly, S., McLenachan, P.A., Lockhart, P.J., 2009. A statistical approach for distinguishing hybridization and incomplete lineage sorting. Am. Nat. 174, E54–E70.
Jones, G., Barlow, K.E., 2004. Cryptic species of echolocating bats. In: Thomas, J.A., Moss, C.F., Vater, M. (Eds.), Echolocation in Bats and Dolphins. University of Chicago Press, Chicago, pp. 345–349.
Khonsue, W., Thirakhupt, K., 2001. A checklist of the amphibians in Thailand. Trop. Nat. History 1, 69–82.
Kimura, M., 1980. A simple method for estimating evolutionary rates of base substitutions through comparative studies of nucleotide sequences. J. Mol. Evol. 16, 111–120.
Kurabayashi, A., Matsui, M., Belabut, D.M., Yong, H.S., Ahmad, N., Sudin, A., Kuramoto, A., Hamidy, A., Sumida, M., 2011. From Antarctica or Asia? New colonization scenario for Australian-New Guinean narrow mouth toads suggested from the findings on a mysterious genus Gastrophrynoides. BMC Evol. Biol. 11 (1), 175.
Li, C., Guo, X.-G., Wang, Y.-Z., 2011. Tadpole types of Chinese megophryid frogs (Anura: Megophryidae) and implications for larval evolution. Curr. Zool. 57, 93–100.
Li, Y.-L., Jin, M.-J., Zhao, J., Liu, Z.-Y., Wang, Y.-Y., Pang, H., 2014. Description of two new species of the genus *Megophrys* (Amphibia: Anura: Megophryidae) from Heishiding Nature Reserve, Fengkai, Guangdong, China, based on molecular and morphological data. Zootaxa 3795, 449–471.
Mahony, S., Foley, N.M., Biju, S., Teeling, E.C., 2017. Evolutionary history of the Asian Horned Frogs (Megophryinae): integrative approaches to timetree dating in the

absence of a fossil record. Mol. Biol. Evol. 34, 744–771.
Mahony, S., Sengupta, S., Kamei, R.G., Biju, S., 2011. A new low altitude species of *Megophrys* Kuhl and van Hasselt (Amphibia: Megophryidae), from Assam, Northeast India. Zootaxa 3059, 36–46.
Narins, P.M., 1983. Divergence of acoustic communication systems of two sibling species of eleutherodactylid frogs. Copeia 1089–1090.
Ohler, A., 2003. Revision of the genus *Ophryophryne* Boulenger, 1903 (Megophryidae) with description of two new species. Alytes 21, 23–44.
Orlov, N.L., Poyarkov Jr, N.A., Nguyen, T.T., 2015. Taxonomic notes on Megophrys frogs (Megophryidae: Anura) of Vietnam, with description of a new species. Russ. J. Herpetol. 22.
Pons, J., Barraclough, T.G., Gomez-Zurita, J., Cardoso, A., Duran, D.P., Hazell, S., Kamoun, S., Sumlin, W.D., Vogler, A.P., 2006. Sequence-based species delimitation for the DNA taxonomy of undescribed insects. System. Biol. 55, 595–609.
Poyarkov Jr, N., Duong, T., Orlov, N., Gogoleva, S., Vassilieva, A., Nguyen, L., Nguyen, V., Nguyen, S., Che, J., Mahony, S., 2017. Molecular, morphological and acoustic assessment of the genus *Ophryophryne* (Anura, Megophryidae) from Langbian Plateau, southern Vietnam, with description of a new species. ZooKeys 672, 49–120.
Program, B.R., 2014. Raven Pro: interactive sound analysis software. Version 1.5. The Cornell Lab of Ornithology Ithaca, New York, USA.
Puillandre, N., Lambert, A., Brouillet, S., Achaz, G., 2012. ABGD, Automatic Barcode Gap Discovery for primary species delimitation. Mol. Ecol. 21, 1864–1877.
Pyron, R.A., Wiens, J.J., 2011. A large-scale phylogeny of Amphibia including over 2800 species, and a revised classification of extant frogs, salamanders, and caecilians. Mol. Phylogenet. Evol. 61, 543–583.
Pyron, R.A., 2014. Biogeographic analysis reveals ancient continental vicariance and recent oceanic dispersal in amphibians. Syst. Biol. 63 (5), 779–797.
Rabosky, D.L., Donnellan, S.C., Grundler, M., Lovette, I.J., 2014a. Analysis and visualization of complex macroevolutionary dynamics: an example from Australian scincid lizards. Syst. Biol. 63, 610–627.
Rabosky, D.L., Grundler, M., Anderson, C., Shi, J.J., Brown, J.W., Huang, H., Larson, J.G., 2014b. BAMMtools: an R package for the analysis of evolutionary dynamics on phylogenetic trees. Methods Ecol. Evol. 5, 701–707.
Rabosky, D.L., Santini, F., Eastman, J., Smith, S.A., Sidlauskas, B., Chang, J., Alfaro, M.E., 2013. Rates of speciation and morphological evolution are correlated across the largest vertebrate radiation. Nat. Commun. 4, 1958.
Rambaut, A., Grass, N.C., 1997. Seq-Gen: an application for the Monte Carlo simulation of DNA sequence evolution along phylogenetic trees. Comput. Appl. Biosci.: CABIOS 13, 235–238.
Rannala, B., Yang, Z., 2003. Bayes estimation of species divergence times and ancestral population sizes using DNA sequences from multiple loci. Genetics 164, 1645–1656.
Rannala, B., Yang, Z., 2013. Improved reversible jump algorithms for Bayesian species delimitation. Genetics 194, 245–253.
Rao, D., Yang, D., 1997. The karyotypes of Megophryinae (Pelobatidae) with a discussion on their classification and phylogenetic relationships. Asiatic Herpetol. Res. 7, 93–102.
Renoult, J.P., Kjellberg, F., Grout, C., Santoni, S., Khadari, B., 2009. Cyto-nuclear discordance in the phylogeny of Ficus section Galoglychia and host shifts in plant-pollinator associations. BMC Evol. Biol. 9, 248.
Ronquist, F., Teslenko, M., Van Der Mark, P., Ayres, D.L., Darling, A., Höhna, S., Larget, B., Liu, L., Suchard, M.A., Huelsenbeck, J.P., 2012. MrBayes 3.2: efficient Bayesian phylogenetic inference and model choice across a large model space. Syst. Biol. 61, 539–542.
Roelants, K., Gower, D.J., Wilkinson, M., Loader, S., Biju, S.D., Guillaume, K., Moriau, L., Bossuyt, F., 2007. Global patterns of diversification in the history of modern amphibians. Proc. Natl. Acad. Sci. 104 (3), 887–892.
Satler, J.D., Carstens, B.C., Hedin, M., 2013. Multilocus species delimitation in a complex of morphologically conserved trapdoor spiders (Mygalomorphae, Antrodiaetidae, Aliatypus). Syst. Biol. 62, 805–823.
San Mauro, D., Vences, M., Alcobendas, M., Zardoya, R., Meyer, A., 2005. Initial diversification of living amphibians predated the breakup of Pangaea. Am. Nat. 165 (5), 590–599.
Schönrogge, K., Barr, B., Wardlaw, J.C., Napper, E., Gardner, M.G., Breen, J., Elmes, G.W., Thomas, J.A., 2002. When rare species become endangered: cryptic speciation in myrmecophilous hoverflies. Biol. J. Linn. Soc. 75, 291–300.
Shen, X.X., Liang, D., Feng, Y.J., Chen, M.Y., Zhang, P., 2013. A versatile and highly efficient toolkit including 102 nuclear markers for vertebrate phylogenomics, tested by resolving the higher level relationships of the Caudata. Mol. Biol. Evol. 30, 2235–2248.
Silvestro, D., Michalak, I., 2012. raxmlGUI: a graphical front-end for RAxML. Org. Divers. Evol. 12, 335–337.
Sukumaran, J., Knowles, L.L., 2017. Multispecies coalescent delimits structure, not species. Proc. Natl. Acad. Sci. 114, 1607–1612.
Tamura, K., Stecher, G., Peterson, D., Filipski, A., Kumar, S., 2013. MEGA6: molecular evolutionary genetics analysis version 6.0. Mol. Biol. Evol. 30, 2725–2729.
Wang, Y.-Y., Zhang, T.-D., Zhao, J., Sung, Y.-H., Yang, J.-H., Pang, H., Zhang, Z., 2012. Description of a new species of the genus *Xenophrys* Günther, 1864 (Amphibia: Anura: Megophryidae) from Mount Jinggang, China, based on molecular and morphological data. Zootaxa 3546, 53–67.
Wang, Y., Zhao, J., Yang, J., Zhou, Z., Chen, G., Liu, Y., 2014. Morphology, molecular genetics, and bioacoustics support two new sympatric *Xenophrys* toads (Amphibia: Anura: Megophryidae) in Southeast China. PloS one 9, e93075.
Wiens, J.J., 2007. Species delimitation: new approaches for discovering diversity. Syst. Biol. 56, 875–878.
Xie, F., Lau, M.W.N., Stuart, S.N., Chanson, J.S., Cox, N.A., Fischman, D.L., 2007. Conservation needs of amphibians in China: a review. Sci. China, Ser. C Life Sci. 50, 265–276.
Yang, Z., 2007. PAML 4: phylogenetic analysis by maximum likelihood. Mol. Biol. Evol. 24, 1586–1591.
Yang, Z., 2015. The BPP program for species tree estimation and species delimitation. Curr. Zool. 61, 854–865.
Yang, Z., Rannala, B., 2010. Bayesian species delimitation using multilocus sequence data. Proc. Natl. Acad. Sci. 107, 9264–9269.
Yu, Y., Harris, A.J., Blair, C., He, X., 2015. RASP (Reconstruct Ancestral State in Phylogenies): a tool for historical biogeography. Mol. Phylogenet. Evol. 87, 46–49.
Zhang, J., Kapli, P., Pavlidis, P., Stamatakis, A., 2013. A general species delimitation method with applications to phylogenetic placements. Bioinformatics 29, 2869–2876.
Zhang, Y., Li, G., Xiao, N., Li, J., Pan, T., Wang, H., Zhang, B., Zhou, J., 2017. A new species of the genus Xenophrys (Amphibia: Anura: Megophryidae) from Libo County, Guizhou, China. Asian Herpetol. Res. 8 75-+.
Zhao, J., Yang, J., Chen, G., Chen, C., Wang, Y., 2014. Description of a new species of the genus *Brachytarsophrys* Tian and Hu, 1983 (Amphibia: Anura: Megophryidae) from southern China based on molecular and morphological data. Asian Herpetol. Res. 5, 150–160.
Zhu, B., Kidd, W.S., Rowley, D.B., Currie, B.S., Shafique, N., 2005. Age of initiation of the India-Asia collision in the east-central Himalaya. J. Geol. 113, 265–285.